Cobalt(II), Nickel(II) and Zinc(II) complexes based on DHA: Synthesis, X-ray crystal structure, antibacterial activity and DFT computational studies

Amel Marir, Toma Nardjes Mouas, Barkahem Anak, Erwann Jeanneau, Amel Djedouani, Louisa Aribi-Zouioueche, Franck Rabilloud

▶ **To cite this version:**

Amel Marir, Toma Nardjes Mouas, Barkahem Anak, Erwann Jeanneau, Amel Djedouani, et al.. Cobalt(II), Nickel(II) and Zinc(II) complexes based on DHA: Synthesis, X-ray crystal structure, antibacterial activity and DFT computational studies. Journal of Molecular Structure, 2020, 1217, pp.128353. 10.1016/j.molstruc.2020.128353 . hal-02869449

HAL Id: hal-02869449
https://hal.science/hal-02869449

Submitted on 20 May 2022

HAL is a multi-disciplinary open access archive for the deposit and dissemination of scientific research documents, whether they are published or not. The documents may come from teaching and research institutions in France or abroad, or from public or private research centers.

L'archive ouverte pluridisciplinaire **HAL**, est destinée au dépôt et à la diffusion de documents scientifiques de niveau recherche, publiés ou non, émanant des établissements d'enseignement et de recherche français ou étrangers, des laboratoires publics ou privés.

Distributed under a Creative Commons Attribution - NonCommercial 4.0 International License

Version of Record: https://www.sciencedirect.com/science/article/pii/S0022286020306785
Manuscript_346210fd2938de152a7de837eeffcbc9

Cobalt(II), Nickel(II) and Zinc(II) Complexes Based on DHA: Synthesis, X-ray Crystal Structure, Antibacterial Activity and DFT Computational Studies

Amel Marir[a], Toma Nardjes Mouas[b], Barkahem Anak[c,d], Erwann Jeanneau [e], Amel Djedouani[d,f*], Louisa Aribi-Zouioueche[a], Franck Rabilloud[g*]

[a]Laboratoire de catalyse asymétrique écocompatible (LCAE). Université Badji Mokhtar Annaba. B.P 12, 23000, Annaba, Algérie
[b]Laboratoire d'Obtention des Substances Thérapeutiques (LOST), Université Constantine 1, 25000, Algérie
[c]Laboratoire de Chimie des Matériaux, Université Constantine 1, 25000, Algérie
[d]Ecole Normale Supérieure de Constantine, Université Constantine 3, 25000, Algérie
[e]Université de Lyon , Centre de Diffractométrie Henri Longchambon, Villeurbanne, France
[f]Laboratoire de Physicochimie Analytique et Cristallochimie des Matériaux Organométalliques et Biomoléculaires, Université Constantine 1, 25000, Algérie
[g]Université de Lyon, F-69003, Lyon, France; Université Lyon 1, Villeurbanne; CNRS UMR5306, Institut Lumière Matière, France

ABSTRACT

In the present work, a combined experimental and computational study of three new DHA chelates namely [Co(DHA)$_2$.2DMSO] (1), [Ni(DHA)$_2$.2DMF] (2) and [Zn(DHA)$_2$.2DMF] (3), (DHA = 3-Acetyl-4-hydroxy-6-methyl-2-oxo-2H-pyran) is reported. Synthesized compounds are characterized by FT-IR which indicates the metal coordination via both oxygen atom, while single-crystal X-ray crystallography confirms the chelates structure as mononuclear complexes having a distorted octahedral coordination geometry of type MO_6 with intermolecular C–H···O bonds. Structures and electronic properties investigated in the framework of the density functional theory (DFT) are in good agreement with experimental results. Besides, a comparative evaluation of *in vitro* antibacterial potential of DHA and derivatives exhibits better results for DHA free ligand, even close to the effect of antibiotics used as references, highlighting the role of hydroxyl function in case of this application.

KEYWORDS

Dehydroacetic acid; Cobalt(II), Nickel(II), Zinc(II) complexes; X-ray crystal structure; antibacterial activity; DFT calculations.

© 2020 published by Elsevier. This manuscript is made available under the CC BY NC user license
https://creativecommons.org/licenses/by-nc/4.0/

1.Introduction

The multifarious role of transition metal complexes in biochemistry has stimulated great interest in the synthesis of new chelates with donor groups, due to the wide range of pharmacological activities of such compounds [1-3]. Mixed *d*-transition metal–ß-diketone compounds were used extensively as starting materials in metallo-cene chemistry [4]. Dehydroacetic acid (DHA = 3-acetyl-4-hydroxy-6-methyl-2H-pyran-2- one) [5], derived from pyrone, or isolated from natural sources (*Solandra nitida*) [6,7], is a versatile starting material for the synthesis of a wide variety of heterocyclic ring systems [8-10]. While the pharmacology and toxicology of DHA have been carefully studied [11], this compound is used as a food additive [12-14], a stabilizer for cosmetics and pharmaco kinetic products [15,16], an antiseptic agent [17,18], an herbicide [19], and it is also used as a plasticizer in a variety of synthetic resins [20]. Furthermore, studies have shown that similar structural analogs and their chelates have a very interesting biological properties [21-24]. For example, Ru(II) and Ru(III) complexes of dehydroacetic acid have been explored for their biological activities such as DNA-binding, antibacterial and antifungal activities [25-26]. This has motivated the present study on the synthesis and structural characterization of dehydroacetic acid complexes as potent antibacterial agents. Our comparative study exhibits the role of the structure on the activity performance.

The present paper reports the synthesis, characterization, and antibacterial potential of DHA based cobalt(II), Nickel(II) and Zinc(II) chelates. Several physicochemical analyses were used including FT-IR spectroscopy and single-crystal X-ray analysis. Computational studies in the framework of the density-functional theory (DFT) were performed in order to rationalize the experimental results and structural properties.

2. Experimental

2.1Measurements and materials

Chemicals were purchased from commercial sources and, unless specified, were used without further purification. Melting points were determined with a digital melting point apparatus using capillary technique. Infrared (IR) spectra were recorded with a Shimadzu FTIR-8010M spectrometer between 400 and 4000 cm^{-1} (KBr disks).

2.2 Crystallographic analyses

Suitable crystals were selected and mounted on a Gemini kappa-geometry diffractometer (Rigaku OD, 2018) equipped with an Atlas CCD detector and using Mo radiation ($\lambda = 0.71073$ Å).

Intensities were collected at 150 K by means of the CrysalisPro software [27]. Reflection indexing, unit-cell parameters refinement, Lorentz-polarization correction, peak integration and background determination were carried out with the CrysalisPro software [27]. An analytical absorption correction was applied using the modeled faces of the crystal [28]. The resulting set of *hkl* was used for structure solution and refinement. The structure was solved with the ShelXT [29] structure solution program using the Intrinsic Phasing solution method and by using Olex2 [30] as the graphical interface. The model was refined with version 2018/3 of ShelXL [31] using Least Squares minimization. The DIAMOND package and Mercury for Windows programs were used for generating figures of structures[32,33].

2. 3. Computational details

Geometries of DHA, and derivatives [$Co(DHA)_2$.2DMSO] (1), [$Ni(DHA)_2$.2DMF] (2) and [$Zn(DHA)_2$.2DMF] (3) were optimized using the range-separated hybrid CAM-B3LYP functional [34]. Co, Ni and Zn atoms were described though relativistic core potentials (ECPs) and associated basis sets [35], while the 6-31G+(d) basis sets were used for other atoms (N, O, S, C, H) [36]. Harmonic frequency analysis was performed to guarantee that optimized structures are local minima. All calculations have been performed using the Gaussian 09 program package [36].

2.4. In vitro antibacterial activity

The title compounds (DHA and metallocomplexes derivatives 1-3), were screened *in vitro* to evaluate their antibacterial activity against four referential strains, *Escherichia coli* ATCC 25922, *Pseudomonas aeruginosa* ATCC 27853 and *Klebsiella pneumonia* ATCC 700603 Gram-negative, *Staphylococcus aureus* ATCC 25923 Gram-positive, using the disc diffusion method [37-39].

Sterilized Petrie dishes were filled with a Muller-Hinton agar medium, then, 100 µl of bacterial inoculums at 0,5 $\times 10^6$ CFU ml^{-1} turbidity concentration were applied on plates surface using sterilized swab. Discs are impregnated with 10 µl of the synthesized compounds at 25mg/ml in DMSO concentration and put on the medium surface, a disc with only DMSO was used as negative control. The plates were incubated 24 h at 37°C, afterward, diameters of zones inhibition were measured in millimeters (mm). All sample tests were performed in triplicate measurements to obtain mean standard deviation (S.D) values.

Investigations on Minimum inhibitory concentration (MIC) values were carried on by a micro dilution method using liquid Mueller-Hinton medium. For this, intermediates concentrations from 12.5 mg/ml to 0.78 mg/ml were obtained by semi-logarithmic dilutions of reason 2, then the dilutions tubes were inoculated by 20 µl of bacterial suspension (0,5 $\times 10^6$ CFU. ml^{-1}), and 280 µl of liquid MH were added to all tubes, the final concentrations of tested compounds in tubes are from

3.125 to 0.195 mg/ml (Table 1). The tubes were incubated 24 h at 37°C [40]. MIC value is considered to be the lowest concentration that inhibits the ocular growth of bacteria after incubation of 24h.

The minimum bacterial concentration (MBC) value is the lowest synthesized compounds concentration that killed 99, 9% of tested bacteria. The MBC test was added to complete the MIC test, as the tested compounds showed a great turbidity in solution. For this swab, striations of the obtained dilutions were applied on agar MH plates, with witness plates without antibiotics, besides a series of dilutions: 1/10, 1/100, 1/1000, 1/10000 of the different tested bacterial inoculums at 0.5×10^6 CFU ml^{-1}. The turbidity concentration was sub cultured using striations on solid MH medium for comparison. All essays were incubated 24 h at 37°C [41].

Table 1. Dilution technique in liquid medium

N° Tubes	Volume of added antibiotic	Intermediate concentration (mg/ml)	Supplemental volume MH (µl)	Inoculum (µl)	Final concentration (mg/ml)
1	100 µl of the solution 25 mg/ml	12.5	280	20	3.125
2	100 µl of the solution 12.5 mg/ml	6.25	280	20	1.562
3	100 µl of the solution 6.25 mg/ml	3.125	280	20	0.781
4	100 µl of the solution 3.12 mg/ml	1.56	280	20	0.39
5	100 µl of the solution 1.56 mg/ml	0.78 mg/ml	280 µl	20 µl	0.195

2.5. Synthesis of complexes

General procedure: To a solution of 2 equiv of DHA dissolved in acetone, 1 equiv of the appropriate metal salt was added. The solution was stirred at room temperature for 1h30min for complexes of Co and Ni, and 6h for Zn complex. The resulting solid was recovered by filtration and washed with cold water, then dried in air. Suitable crystals for X-ray diffraction were collected by slow evaporation at room temperature from dimethylsulfoxyde for Co(II) and dimethylformamide for Ni(II) and Zn(II) complexes.

3. Results and discussion

The synthesis of complexes (Scheme 1) was carried out at room temperature by addition of the appropriate salts (1 equiv. to 2 equiv. of DHA). The synthesized complexes are solids, air stable and do not require special precautions for storage. They are all poorly soluble in organic solvents such as ethanol, methanol and n-butanol. But they are all soluble in dimethylsulfoxide (DMSO) and dimethylformamide (DMF). The molecular structures of complexes were characterized by IR and single crystal X-ray diffraction analysis.

Bis(3-acetyl-6-methyl-2-oxo-2H-pyran-4-olato)bis(dimethyl sulfoxide) cobalt(II)
$[Co(DHA)_2.2DMSO]$ (1). Yield 88%, mp > 260°C, pink solid. IR spectrum, ν, cm^{-1}:1670 (C=O, lactones), 1625 (C=O, acetyl), 3377 (C-O, hydroxyl), 595 (O-M), 1050 (C-O-C).

Bis(3-acetyl-6-methyl-2-oxo-2*H*-pyran-4-olato)bis(dimethyl formamide) nickel(II)
$[Ni(DHA)_2.2DMF]$ **(2)**. Yield 80%, mp=243°C, green solid, IR spectrum, ν, cm–1:1667 (C=O, lactones), 1583 (C=O, acetyl), 3377 (C-O, hydroxyl), 600 (O-M), 1010 (C-O-C).
Bis(3-acetyl-6-methyl-2-oxo-2*H*-pyran-4-olato)bis(dimethyl formamide) zinc(II)
$[Zn(DHA)_2.2DMF]$ **(3).** Yield: 93%, mp=178°C, white solid, IR spectrum, ν, cm^{-1}:1670 (C=O, lactones), 1575 (C=O, acetyl), 3377 (C-O, hydroxyl), 620 (O-M), 1000 (C-O-C).

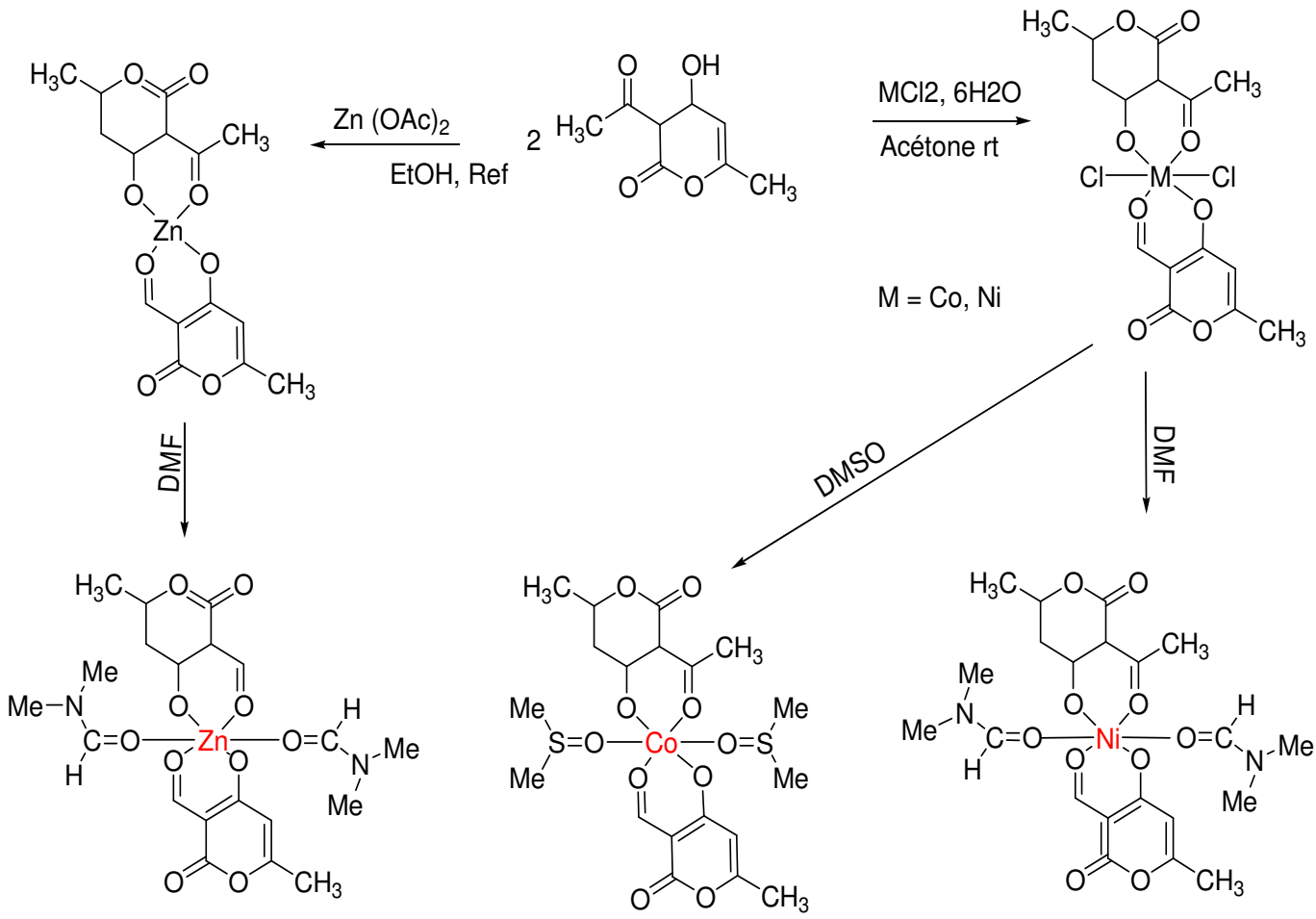

Scheme 1. Synthesis of metal complexes.

3.1 Infrared spectra

DHA ligand has a strong band in the range 1734-1581 cm^{-1} corresponding to the υ(C_4=O) lactones stretching frequency (Figure 1). The band observed around 1680 cm^{-1} is assigned to υ(C=O) acetyl of DHA. This strong band is shifted to a higher wave in the spectra of metal (II) complexes. This indicates the coordination of keto (C=O) and (C-$O_{(hydroxyl)}$) groups to the metal atom in complexes. In the spectra of the complexes, the appearance of new bands in the region 600-550 cm^{-1} can be attributed to M-O bands [1,49].

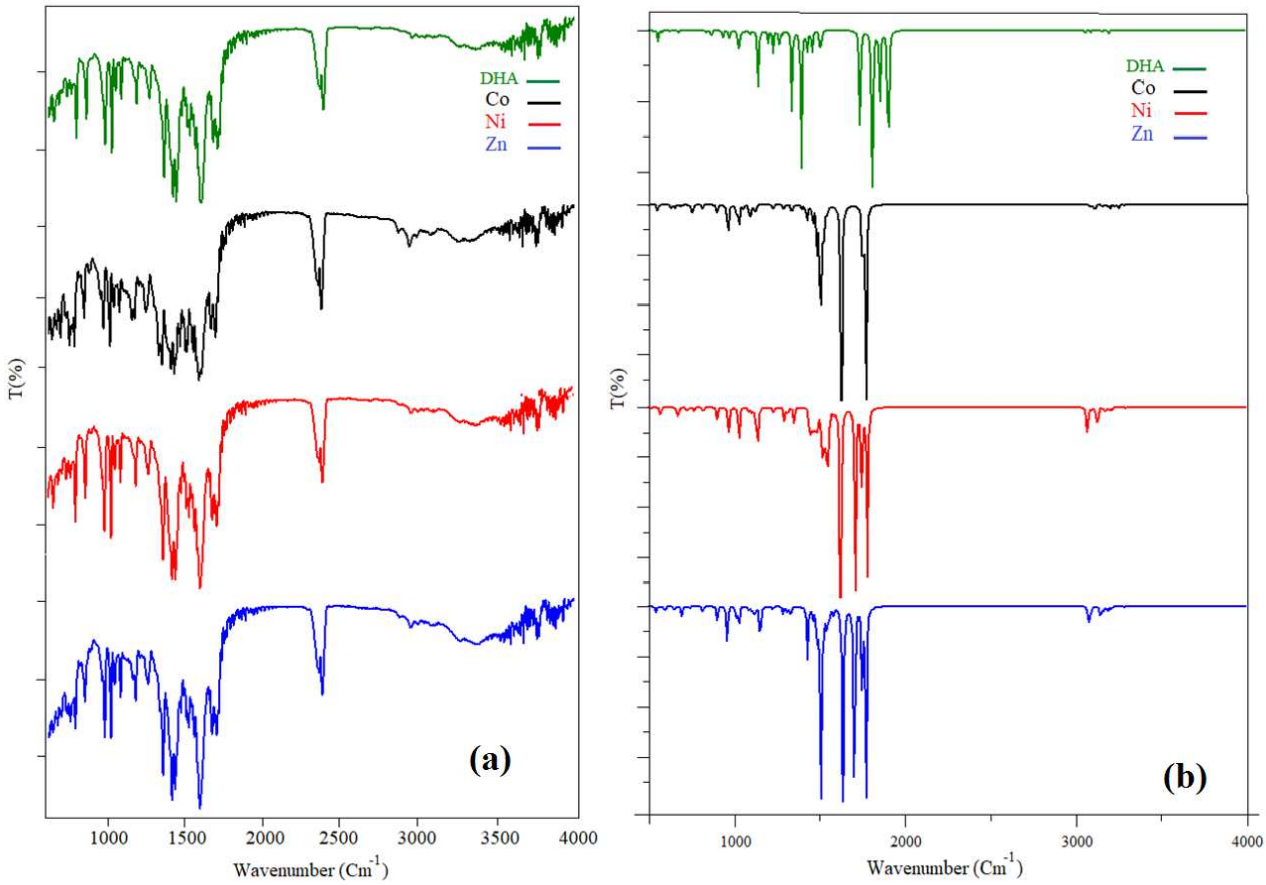

Figure 1. Experimental (a) and theoretical (b) infrared spectra of DHA, [Co(DHA)$_2$.2DMSO], [Ni(DHA)$_2$.2DMF] and [Zn(DHA)$_2$.2DMF] complexes.

3.2 Crystallographic studies

The crystals of molecules were grown in DMSO or DMF solution through slow evaporation process, then suitable crystals were collected and analyzed through single crystal X-rays diffraction analysis. Compound (**1**) crystallized in a monoclinic system, P2$_1$/c space group with two units per cell (Z = 2), whereas (**2**) and (**3**) crystallized in a triclinic system P-1 space group with two units per cell (Z = 2) too. The main crystal parameters are reported in Table 2. Some selected bond distances and angles are listed in Table 3. The asymmetric unit of the three complexes contains one independent molecule. The numbering schema and displacement ellipsoid plot of (1), (2), (3) are shown in Figure 2.

In the structure of the mononuclear complexes, the Co^{II}, Ni^{II} and Zn^{II} atoms lie on an inversion center and have a distorted octahedral coordination geometry of type MO_6. The bidentate dehydroacetic acid (DHA) ligands occupy the equatorial plane of the complexes in a *trans* configuration, each chelating the metal through two oxygen atoms, while the

dimethylsulfoxide (DMSO) for Co(II) and dimethylformamide (DMF) for Ni and Zn molecules fill the two axial sites via their oxygen atom. The average bond lengths and bond angles parameters of complexes are in the normal ranges [24, 42-44]. The bond lengths of M–O in three complexes are close to each other (Table 3). In the crystalline structure of (1), the cations and anions are arranged in the layers parallel to the (010) plane along the *b* axis (Figure 3(a)). In (2) and (3), the crystal packing can be described as double layers, planes along the *b* axis (Figure 3(b)) and (c)). All The complexes present intermolecular C–H···O bonds (Table 4).

Table 2. Crystallographic data and structure refinement details for complexes 1, 2 and 3.

Compound	**(1)**	**(2)**	**(3)**
Empirical formula	$C_{20}H_{26}CoO_{10}S_2$	$C_{22}H_{28}N_2O_{10}Ni$	$C_{22}H_{28}N_2O_{10}Zn$
Formula weight, g/mol	549.46	539.17	545.83
Crystal description	Needle	Needle	Plate
Space group	$P2_1/n$	P-1	P-1
Crystal system	Monoclinic	Triclinic	Triclinic
F(000)	570	282	284
Refinement method	full-matrix least-squares on F^2		
a/Å	11.2686(13)	7.6695(7)	7.6695(7)
b/Å	6.2346(9)	8.1780(9)	8.1780(9)
c/Å	16.412(2)	9.5238(9)	9.5238(9)
α/°	90	84.416(8)	84.416(8)
β /°	92.966(11)	86.543(7)	86.543(7)
γ/°	90	77.522(8)	77.522(8)
V/Å^3	1151.5(3)	579.99(10)	579.99(10)
Z	2	1	1
Temperature/K	100.00(10)	100.00(10)	100.00(10)

θ Range for data collection (°)	3.496–29.658	3.199-29.689	3.199-29.689
Radiation	Mo Kα(λ= 0.71073)	Mo Kα(λ= 0.71073)	Mo Kα(λ= 0.71073)
Dcalcd (g/cm^{-3})	1.585	1.563	1.563
Range/indices (h, k, l)	-15≤ h ≤14-7≤ k ≤8 22≤ l ≤20	-10 ≤ h ≤10 -11 ≤ k ≤11 --12 ≤ l ≤13	-10 ≤ h ≤10 -11 ≤ k ≤10 --13≤ l ≤13
Ref Nmb of reflections measured	13703	15294	15294
independent reflections	2966	2942	2985
Reflections with I > 2σ(I)	2442	2411	2735
Number of parameters	155	164	165
Absorptioncoefficient(mm^{-1})	0.981	1.120	1.120
Goodness-of-fit (GOF)	1.086	1.049	1.121
wR(F2)	0.1253	0 .1211	0.0924
Rint	0.0515	0.0515	0.0392
Max / min δp (e /Å^3)	0.122 /−1.171	0.105/-0.860	0.614/-0.860

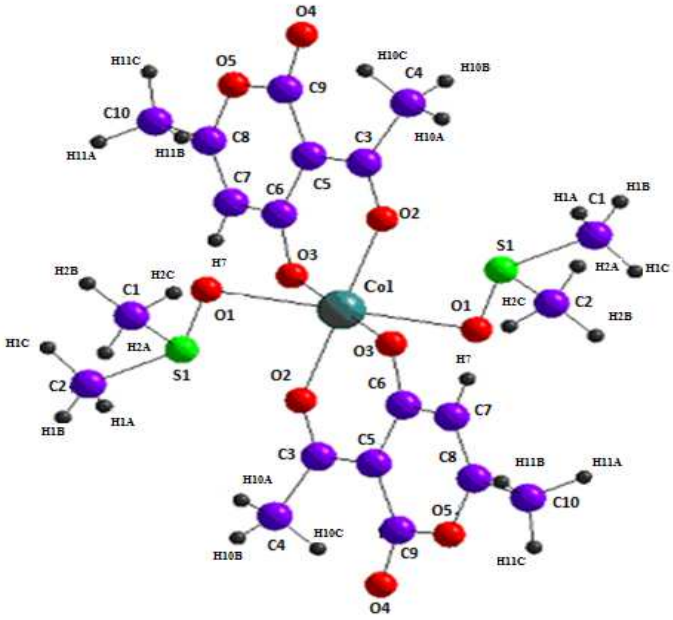
O4
H11C
O5
H10C
C4
H10B
C9
C10
C8
C3
H11A
H11B
H10A
C7
C6
C5
O2
H1A
C1
H1B
S1
H7
O3
H2B
H2C
Co1
H2A
H1C
C2
O1
H2C
C1
O1
S1
H1C
H2A
O3
C2
H7
O2
C6
H1B
H1A
C7
C5
C3
C8
H11B
H11A
H10A
C10
O5
H10C
C4
C9
H10B
H11C
O4

(1)

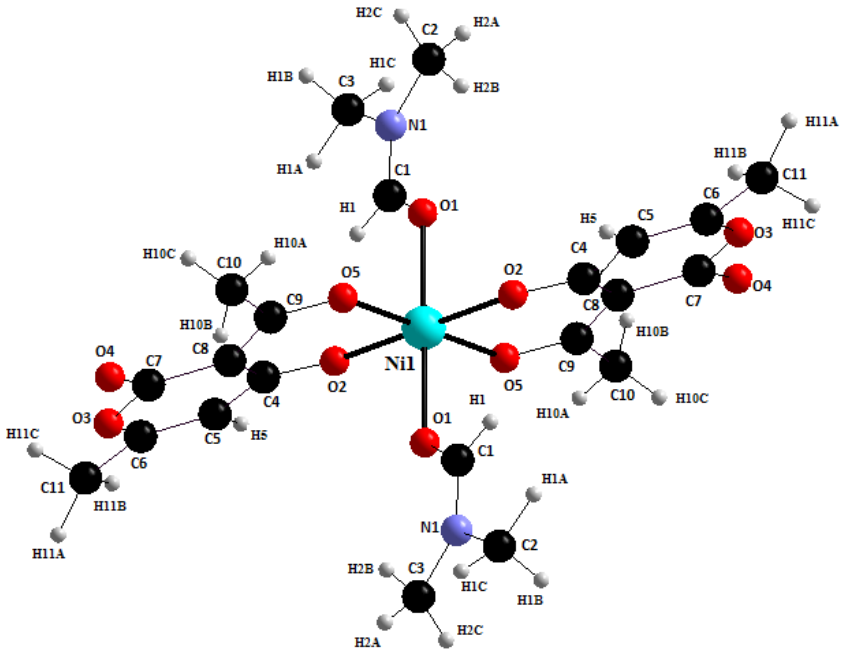
H2C
C2
H2A
H1C
H1B
C3
H2B
N1
H1A
C1
H11A
H11B
C11
H1
O1
C6
H5
C5
H11C
O3
C4
O2
O5
C10
H10C
H10A
C9
C8
C7
O4
H10B
H10B
O4
C7
C8
Ni1
C9
C10
H10A
H10C
O2
C4
O3
O5
H1
C5
H5
O1
H11C
C6
C1
C11
H11B
H1A
H11A
N1
C2
H2B
C3
H1C
H1B
H2A
H2C

(2)

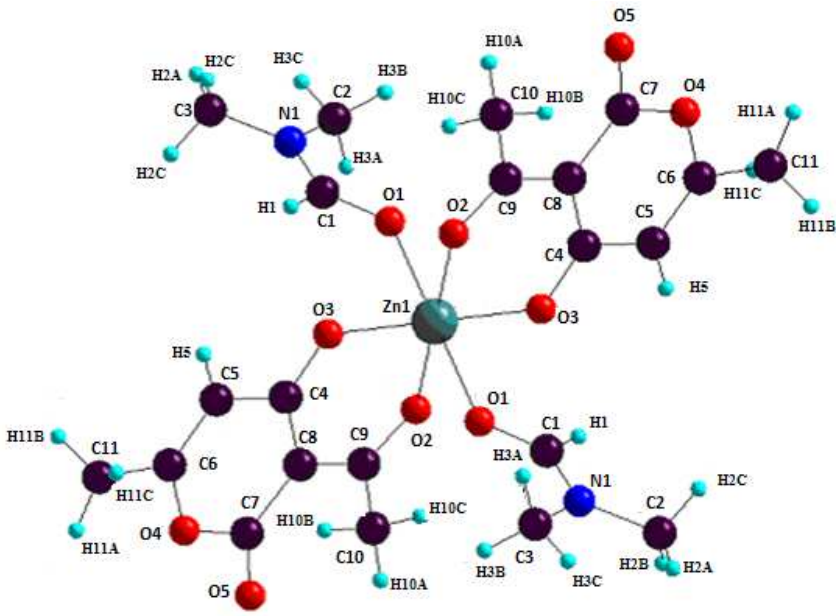

(3)

Figure 2. View of the molecular structure of (1-3) complexes.

Table 3. Selected bond distances (Å) and angles (°) for DHA chelates.

Bond	**Bond lengths (Å)**	**Bond Angle**	**Angle(°)**
(1)			
Co1– O1 Co1–O2 Co1– O3	2.1487(19) 2.0506(17) 2.0080(19)	O2–Co1– O2 O2–Co1– O1 O2–Co1– O1 O3–Co1– O2 O3–Co1– O2 O3–Co1– O3 O3–Co1– O1 O3–Co1– O1 O1–Co1– O1 C3–O2– Co1 C6–O3– Co1 S1–O1– Co1	180.0 91.30(7) 88.70(7) 94.72(7) 85.28(7) 180.00 89.66(8) 90.34(8) 180.00 132.42(18) 130.63(17) 116.40(11)
(2)			

Ni1–O1 Ni1–O2 Ni1–O5	Ni1– O1 2.090(2) Ni1–O2 1.9858(19) Ni1– O5 2.003(2)	O1–Ni1–O1 O2–Ni1–O1 O2–Ni1– O1 O2–Ni1– O2 O2–Ni1–O5 O2–Ni1– O5 O5–Ni1– O1 O5–Ni1–O1 O5–Ni1–O5 C1–O1–Ni1 C4–O2–Ni1	180.00 91.74(8) 88.26(8) 180.00 87.91(8) 92.09(8) 91.11(8) 88.89(8) 180.00 121.95(18) 127.59(18)
(3)			
Zn1–O1 Zn1– O2 Zn1– O3	2.0122(15) 2.0311(15) 2.1691(17)	O2– Zn1– O2 O2–Zn1–O3 O2–Zn1–O3 O2–Zn1–O1 O2–Zn1–O1 O3–Zn1–O3 O3–Zn1–O1 O3–Zn1–O1 O1–Zn1–O1 C4–O2–Zn1 C9–O3 – Zn1 C1–O1–Zn1	180.00 93.63(6) 86.37(6) 91.56(6) 88.44(6) 180.00 91.22(6) 88.78(6) 180.00 127.98(14) 130.67(14) 121.44(15)

Table 4. Distances (Å) and angles (°) of hydrogen bond for (1), (2) and (3).

D–H…A	d(D–H)	d(H…A)	d(D–A)	D–H–A
(1)				
C1–H1A… O3	0.96	2.47	3.387(4)	160
C1–H1B… O4	0.96	2.50	3.334(4)	145
C2–H2B… O4	0.96	2.50	3.328(4)	144
(2)				
C1–H1…O2	0.93	2.43	3.004(4)	120
C2–H2A…O4	0.96	2.59	3.405(4)	143
C3–H3A…O1	0.96	2.40	2.799(4)	105
(3)				
C1–H1…O2	0.93	2.48	3.063(3)	121

C2–H2A…O5	0.96	2.59	3.430(3)	146
C3–H3A…O1	0.96	2.39	2.795(3)	105

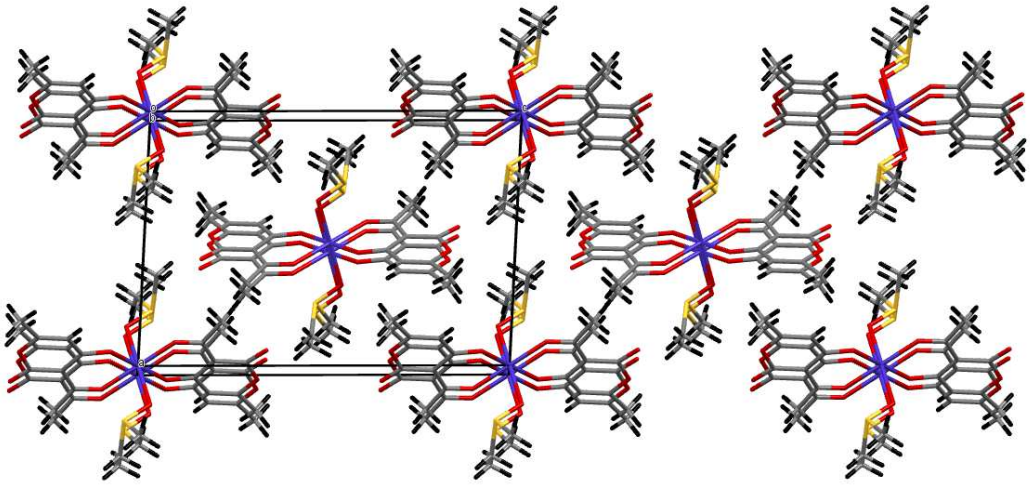

(a)

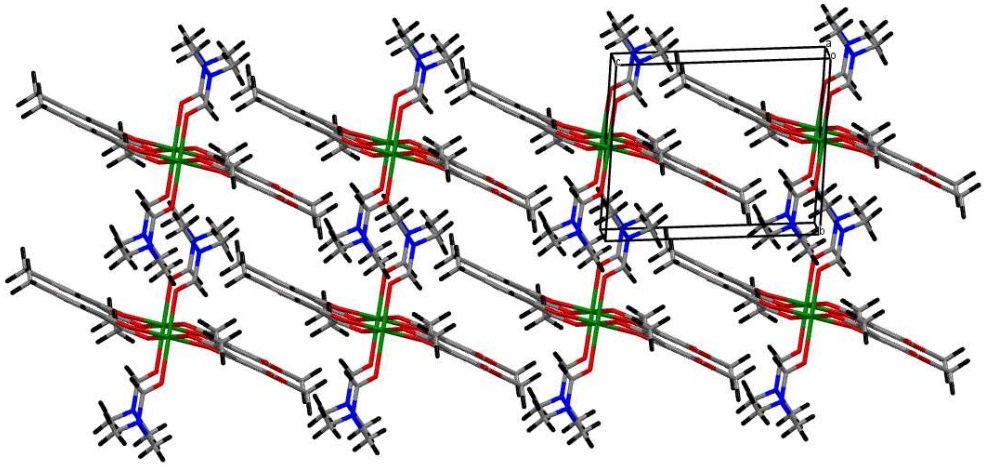

(b)

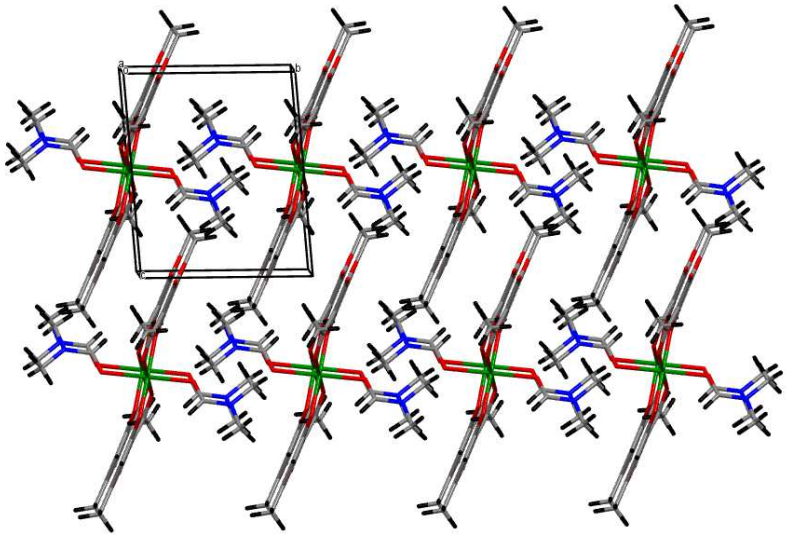

(c)

Figure. 3. (a) View of the crystal structure of (**1**) showing layers in b = 0, ½, and 1; (b) View of the crystal structure of (**2**) showing double layers parallel to (010) plane at c=0 and c=1 along the c axis; (c) View of the crystal structure of (**3**) showing double layers parallel to (010) plane at b=0 and b=1 along the c axis.

3.3. Optimized structure

The optimized structures of [Co(DHA)$_2$.2DMSO] (**1**), [Ni(DHA)$_2$.2DMF] (**2**) and [Zn(DHA)$_2$.2DMF] (**3**) have been calculated at DFT level in the gas phase using the CAMB3LYP density functional. The bonds lengths and angles are reported in Table 5 together with X-ray diffraction data. Calculated values for the complex (**1**) are in good agreement with experimental results. The relative errors of calculated bond lengths are 0.005-0.106 Å and those of angles are 0.12º-3.07º. For complexes (**2**) and (**3**), the calculated bond lengths correlate nicely with experimental values with slight deviations within 0-0.04 Å and 0.128-0.694 Å for (**2**) and (**3**) respectively. The calculated bond angle for (**2**) and (**3**) are similar to the experimental values with deviations within 0.50-5.65º and 1.14-10.38° for (**2**) and (**3**) respectively.

Table 5. Selected bond lengths (Å) and angles (°) calculated at DFT/CAM-B3LYP level for complexes (**1**),(**2**) and (**3**).

	[Co(DHA)$_2$.2DMSO] (**1**)		[Ni(DHA)$_2$.2DMF] (**2**)		[Zn(DHA)$_2$.2DMF] (**3**)	
	CAMB3LYP	Exp.	CAMB3LYP	Exp.	CAMB3LYP	Exp
Bond lengths(Å)						
M1-O1	2.157	2.149	2.784	2.090	2.159	2.169
M1-O2	1.945	2.051	1.848	1.986	2.052	2.012
M1-O3	1.965	2.008	-	-	2.031	2.031
M1-O5	-	-	1.854	2.003	-	-
Angles (°)						
O1-M1-O2	87.53	88.70	90.54	91.72	85.90	91.55
O2-M1-O3	88.40	88.28	-	-	83.63	86.37
O3-M1-O1	92.73	89.66	-	-	89.27	88.77
O2-M1-O5	-	-	91.67	87.91	-	-
O5-M1-O1	-	-	78.50	88.88	-	-

3.4 Vibrational analysis

Intense IR absorption bands of DHA and complexes (**1**), (**2**) and (**3**) are calculated at CAM-B3LYP level and compared to experimental spectra in Figure 1, Table 6 gives major lines. Globally, the calculated values are in good agreement with the experimental data. The value of the υ(C-O)ac band was calculated at 1262 cm^{-1} for free ligand and at 1335, 1311 and 1328 cm^{-1}for complexes (1), (2) and (3) respectively. The calculated value at 1507 cm^{-1} is associated with stretching vibration of υ(C-O), the experimental frequency has been observed at 1550 cm^{-1} for free ligand. The experimental υ(C=O) stretching vibrations are measured at 1642,1625,1583 and 1575 cm^{-1} for DHA, (1), (2) and (3) complexes respectively, while these bands are calculated at 1734, 1626,1582 and 1578 cm^{-1} respectively. The experimental peaks at 1718 cm^{-1} (DHA), 1670 cm^{-1} (1) and (3), 1667 cm^{-1} (2) belong to the ν(C=O$_{Lactone}$) stretching vibrations, and the calculated values are 1734 cm^{-1} (DHA), 1639 cm^{-1}(1), 1674 cm^{-1}(2) and 1667 cm^{-1}(3). These variations of υ(C–O) confirm the participation of the oxygen atom in the coordination [45-48]. The experimental stretching vibration ν(M-O) is measured at 595, 600 and 620 cm^{-1} for complexes (1), (2) and (3) respectively, in agreement with the calculated frequencies of 601, 624 and 636 cm^{-1}. The coordination distances in (1) are in good agreement with those found in four mixed-ligand complexes of Cobalt(II) with general composition [Co(DHA)(L)(H2O)2], where LH= β-ketoenolates, *o*-acetoacetotoluidide (*o*-aatdH), *o*-acetoacetanisidide (*o*-aansH), acetylacetone (acacH) or 1-benzoylacetone (1-*bac*) [46]. For the complex of nickel, the ν(Ni-O) vibrational frequency (experimental and calculated) is comparable with those measured for similar complexes [47]. For ν(Zn-O), it can be envisaged when comparing with N-dehydroacetic acid-glucosamine already described vibrations [49].

Table 6. Selected experimental (between brackets) and calculated vibrational frequencies (cm^{-1}) for DHA and complexes.

Assignment	**DHA**	**[Co(DHA)$_2$.2DMSO](1)**	**[Ni(DHA)$_2$.2DMF](2)**	**[Zn(DHA)$_2$.2DMF](3)**
ν(C-O)ac	1262	1335 **C_3-O_2**	1311 **C_9-O_5**	1328 **C_9-O_2**
(Stretching)	**(1254)**	**(1333)**	**(1300)**	**(1335)**
ν(C-O)	1507	-	-	-
(Stretching)	**(1550)**	-	-	-
ν(C=O)	1734	1626 **C_6-O_3**	1582 **C_4-O_2**	1578 **C_4-O_3**
(Stretching)	**(1642)**	**(1625)**	**(1583)**	**(1575)**
ν(C=$O_{Lactone}$)	1734	1639 **C_9-O_4**	1642 **C_7-O_4**	1636 **C_7-O_5**
(Stretching)	**(1718)**	**(1670)**	**(1667)**	**(1670)**
ν(M-O)	-	601	624	636
(Stretching)	-	**(595)**	**(600)**	**(620)**

3.5 Anti-bacterial activity

Antibacterial potential of new DHA derivatives against four referential strains, *E.coli*, *P.aeruginosa, K. pneumonia, S. aureus,* was evaluated *in vitro* by disc diffusion method using Muller-Hinton agar medium. Results are given in Table 7, together with their graphical representation shown in Figure 4. The obtained zones of inhibition show good to moderate antibacterial activity for title compounds against all tested bacterial strains ; for comparison Gentamicine (10µg /disc), and Nalidixique (30µg/ disc) were used as standards.

Results indicate that all the compounds show moderate to excellent antibacterial activity. Among the compounds, DHA exhibits a high activity against all tested strains, complex (1) shows a very good activity against S. *aureus,* complex (2) gives a moderate activity against all tested bacteria, complex (3) has a very good activity against *K.pneumonia* and *P.aeruginosa* and a moderate one against the other tested bacteria. In general, all synthesized compounds show moderate activity against *E.coli* in comparison with antibiotics used as references. The MBC values reveal that DHA has a bactericidal effect ≤ 0.195 mg/ml on all tested strains, and all synthesized compounds (1)-(3) have nearly the same bactericidal effect (≤0.195 mg/ml) in case of *E.coli* bacteria and have no bactericidal effect on bacteria with lower sensitivity by disc diffusion method (Table8).

Table 7. Antibacterial zone of inhibition (mm) of DHA and complexes (1)-(3). All data are expressed as the means ± standard deviation (SD) of triplicate measurements. NA and GN refer to Nalidixique and Gentamicine respectively.

Coumpounds	*E.coli*	*P.aeruginosa*	*K.pneumonia*	*S. aureus*
DHA	15.00±0.00	20.00±0.50	20.00±0.50	15.00±0.00
(1)	14.00±0.50	12.00±0.00	12.00±0.00	18.00±0.50
(2)	16.00±0.00	10.00±0.00	15.00±0.50	12.00±0.00
(3)	15.00±0.50	15.00±0.50	18.00±0.50	13.00±0.50
NA	42.00	0.00	28.00	22.00
GN	38.00	24.00	18.00	-
DMSO	0.00	0.00	0.00	0.00

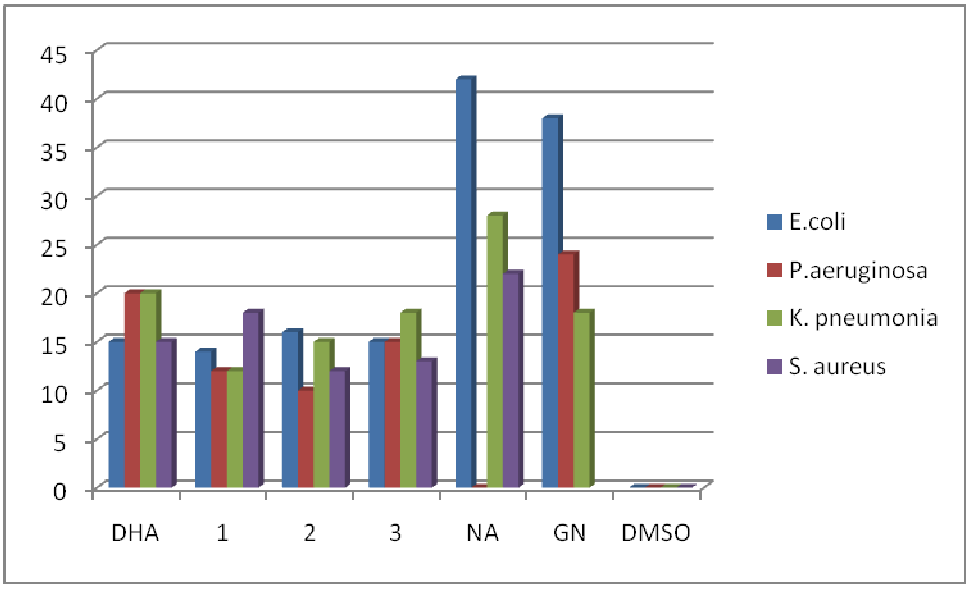

Figure 4. Antibacterial activity of DHA and complexes (1)-(3) against gram-positive and gram-negative bacteria.

Table 8. MIC and MBC (mg/ml) inhibitory values for DHA and derivative complexes (1)-(3).

Coumpounds	*E.coli*		*P.aeruginosa*		*K. pneumonia*		*S. aureus*	
	MIC	MBC	MIC	MBC	MIC	MBC	MIC	MBC
DHA	N.D	≤0.195	N.D	≤0.195	N.D	≤0.195	N.D	≤0.195
1	N.D	N.A	N.D	N.A	N.D	N.A	N.D	N.A
2	N.D	≤0.195	N.D	N.A	N.D	N.A	N.D	N.A
3	N.D	≤0.195	N.D	N.A	N.D	N.A	N.D	N.A

N.A : no activity ; N.D : not possible to detect

4. Conclusions

Three complexes of Co(II), Ni(II), and Zn(II) derived from dehydroacetic acid (DHA) have been successfully synthesized and characterized by single-crystal X-ray analysis and FT-IR spectroscopy. In the structure of the mononuclear complexes, the Co^{II}, Ni^{II} and Zn^{II} atoms lie on an inversion center and have a distorted octahedral coordination geometry of type MO_6. Both bidentate dehydroacetic acid (DHA) ligands occupy the equatorial plane of the complexes in a *trans* configuration, each chelating the metal through two oxygen atoms, while the dimethylsulfoxide (DMSO) for Co(II) and dimethylformamide (DMF) for Ni and Zn molecules, fill the two axial sites via their oxygen atom. FT-IR spectral data of the ligand and metal complexes supported by DFT calculations confirm the structural assignment. The *in vitro* antibacterial potential of DHA and derivatives have been evaluated using the disc diffusion method. The tested compounds exhibited varying degrees of inhibitory effects on the growth of bacterial species compared to referential used antibiotics GN and NA. Results were generally better for the free DHA ligand, probably insured by hydroxyl function.

Acknowledgments

The authors acknowledge the Algerian Ministry of Higher Education and Scientific Research, the Algerian Directorate General for Scientific Research and Technological Development, and Bordj Badji Mokhtar University of Annaba.

References

[1] V. N. Patange, B. R. Arbad, Synthesis, spectral, thermal and biological studies of transition metal complexes of 4-hydroxy-3-[3-(4-hydroxyphenyl)-cryloyl]-6-methyl-2H-pyran-2-one, J. Serb. Chem. Soc., 76 (2011) 1237-1246.

[2] V. N. Patange, R. K. Pardeshi, B.R. Arbad, Transition metal complexes with oxygen donor ligands: a synthesis, spectral, thermal and antimicrobial study, J. Serb. Chem. Soc., 73 (2008) 1073-1082.

[3] S. Tabti, A. Djedouani, D. Aggoun, I. Warad, S. Rahmouni, S. Romdhane, H. Fouzi, New Cu (II), Co(II) and Ni(II) complexes of chalcone derivatives: Synthesis, X-ray crystal structure, electrochemical properties and DFT computational studies, J. Mol. Struct. 1155 (2018) 11-20.

[4] M. E Smith, R. A, Anderson,$Me_5C_5Ni(acac)$: A Monomeric, Paramagnetic, 18-Electron, Spin-Equilibrium Molecule, J. Am. Chem. Soc.118 (1996) 11119–11128.

[5] J. N. Collie, H. R. Le Sueur, Salts of dehydracetic acid, J. Chem. Soc.Trans.65 (1894) 254-262.

[6] C. Rivera, E. Piñeyro, F. Giral, Dehydroacetic acid in anthers of Solandra nitida(Solanaceae), Experientia. 32(12) (1976) 1490-1490.

[7] A. Townshend, D. T. Burns, R. Lobinski, E. J. Newman, G. Guilbault, Z. Marczenko, H. Onishi, Dictionary of Analytical Reagents, 1993,1st Ed, 5.

[8] a) A. El Alami, S. Hamid, A. El Kihel, M. Saadi and L. El Ammarib, 3,3' -[(1 E,1' E)-Hydrazine-1,2-diylidenebis(ethan-1-yl-1-ylidene)]bis(4-hydroxy-6-methyl-2 H-pyran-2-one), Acta Cryst. 4 (2019) x191348. b) M. Salehi, M. Galini, M. Kubicki, A. Khaleghian, Synthesis and Characterization of New Cobalt(III) and Nickel(II) Complexes Derived from Acetylacetone and 2-Aminopyridine: a New Precursor for Preparation of NiO Nanoparticles, Russ. J. Inorg. Chem. 64 (2019) 18–27.

[9] H. Tabuchi, T. Hamamoto, S. Miki, T. Tejima, A. Ichihara, Total Synthesis and Stereochemistry of Alternaric Acid, J. Org. Chem. 59 (1994) 4749-4759.

[10] a) R. Teimuri-Mofrad, K. Rahimpour, M. Gholizadeh, Design, synthesis, characterization and fuorescence property evaluation of dehydroacetic acid-based chalcones, J. Iran Chem. Soc 17 (2020) 1103–1109.

b) E. Martins de Carvalho, R. Ribeiro Riente, J. D. Figueroa Villar, Synthesis and Spectroscopic Determination of the Coordination Differences of Cadmium and Zinc Complexes of Dehydroacetic Acid with Pyridine and γ-Picoline, Acad. J. Chem. 4 (9) 2019 81-89.

[11] H. C. Spencer, V. K. Rowe, D. D. Mc Collister, Dehydroacetic acid. I. Acute and chronic toxicity, J. Pharmacol. 99 (1950) 57-68.

[12] H. W. Rossmoore, Handbook of biocide and preservative use, 1995,1st Ed, 341.

[13] V. O. Sheftel, Indirect Food Additives and Polymers: Migration and Toxicology, 2000 ,1st Ed, 196.

[14] U. S. Yousef, A novel conducting polymer film by electrochemical oxidation of 3-[1-(2-aminophenylimino)-ethyl]-6-methylpyran-2,4-dione schiff base in aqueous medium, Eur. Poly. J. 36 (2000) 1629-1644.

[15] P. V. Rao, A. V. Narasaiah, Synthesis, characterization and biological studies of oxovanadium(IV), manganese(II), iron(II), cobalt(II), nickle(II) and copper(II) complexes derived from a quadridentate ligand, Indian J. Chem. A. 42 (2003) 1896-1899.

[16] L. Zema, M. E. Sangalli, A. Maroni, A. Foppoli, A. Bettero, A. azzaniga, Active packaging for topical cosmetic/drug products: A hot-melt extruded preservative delivery device, Eur. J. Pharm. Biopharm. 75 (2010) 291-296.

[17] U. Kunigoshi, Synthesis of dehydroacetic acid isonicotinyl hydrazone sodium-salt. Its antitubercular effect on clinical tuberculosis, Chemotherapy, 6, (1958) 336-341.

[18] A. A. Kubaisi, K. Z. Ismail, Nickel(II) and palladium(II) chelates of dehydroacetic acid Schiff bases derived from thiosemicarbazide and hydrazinecarbodithioate,Can. J. Chem. 72 (1994) 1785-1788.

[19] S. Jadhav, A. Munde, S. Shankarwar, V. Patharkar, V. Shelke, T. Chondhekar, Synthesis, Potentiometric, Spectral Characterization and Microbial Studies of Transition Metal Complexes with Tridentate Ligand, J. Korean Chem. Soc. 54(2010) 515-522.

[20] A. B. Boese Jr, Diketene A New Industrial Chemical, Ind. Eng. Chem. 32 (1940) 16-22.

[21] M.Z. Chalaca, J.D. Figueroa-Villar, R.A. Ellena E.E. Castellano, Synthesis and structure of cadmium and zinc complexes of dehydroacetic acid, Inorg. Chim. Acta. 328 (2002) 45-52.

[22] S.S.Lim, H.S.Kim, D.U.Lee, In vitro Antimalarial Activity of Flavonoids and Chalcones, Bull. Korean Chem. Soc. 28 (2007) 2495-2497.

[23] M. S. Ponnurengam, S. Malliappan, K. G. Sethu, M. Doble, QSAR Studies on Chalcones and Flavonoids as Anti-tuberculosis Agents Using Genetic Function Approximation (GFA) Method, Pharm. Bull. 55 (2007) 4 4.

[24] G.S.B. Viana, M.A.M. Bandeira, F.J.A. Matos, Analgesic and antiinflammatory effects of chalcones isolated from Myracrodruon urundeuva Allemão, Phytomed,10 (2003) 189-195.

[25] S. F. Tan, K. P. Ang , H. L. Jayachandran, Synthesis and characterisation of copper(II), nickel(II) and palladium(II) complexes of some Schiff bases of dehydroacetic acid, Trans. Met. Chem. 9 (1984) 390-395.

[26] J. Casab, J. Marqijet, M. Moreno-Manad, M. Prior F., Temidor, Transition metal complexes with dehydroacetic acid : Crystal structure of bis(3-acetyl-4-Hydroxy- 6- Methyl-2-pyrone)Cobalt(II) Bis dimethylformamide), Polyhedron. 6 (1987) 1235-1238.

[29] Rigaku Oxford Diffraction, (2018), CrysAlisPro Software system, version 1.171.39.46, Rigaku Corporation, Oxford, UK.

[27] R. C. Clark, J. S. Reid, The analytical calculation of absorption in multifaceted crystals, Acta Cryst. A51 (1995) 887-897

[28] G. M. Sheldrick, ShelXT-Integrated space-group and crystal-structure determination, Acta Cryst. A71 (2015) 3-8.

[29] O.V. Dolomanov, L.J. Bourhis, R.J. Gildea, J.A.K. Howard, H. Puschmann, Olex2: A complete structure solution, refinement and analysis program, J. Appl. Cryst., 42 (2009) 339-341.

[30] G. M. Sheldrick, Crystal structure refinement with ShelXL, Acta Cryst. C27 (2015)3-8.

[31] K.Brandenburg, M.Berndt, DIAMOND, CrystalImpact, Bonn, Germany(2001).

[32] C. F. Macrae, P. R. Edgington, P. McCabe, E. Pidcock, G. P. Shields, R. Taylor, M. Towler, J. Van De Streek, Mercury: visualization and analysis of crystal structures, J. Appl. Cryst. 39 (2006) 453–457.

[33] D. Yanai, D.P. Tew, N.C. Handy, A new hybrid exchange–correlation functional using the Coulomb-attenuating method (CAM-B3LYP), Chem. Phys. Lett. 393 (2004)51-57.

[34] M. Dolg, U. Wedig, H. Stoll, H. Preuss,Energy-adjusted ab initio pseudopotentials for the first row transition elements, J. Chem. Phys. 86 (1987) 866-872.

[35] M.J. Frisch, G.W. Trucks, H.B. Schlegel, G.E. Scuseria, M.A.n Robb, J.R. Cheeseman, G. Scalmani, V. Barone, B. Mennucci, G.A. Petersson, H. Nakatsuji, M. Caricato, X. Li, H.P. Hratchian, A.F. Izmaylov, J. Bloino, G. Zheng, J.L. Sonnenberg, M. Hada, M. Ehara, K. Toyota, R. Fukuda, J. Hasegawa, M. Ishida, T. Nakajima, Y. Honda, O. Kitao, H. Nakai, T. Vreven, J.A. Montgomery, Jr, J.E. Peralta, F. Ogliaro, M. Bearpark, J.J. Heyd, E. Brothers, K.N. Kudin, V.N. Staroverov,R. Kobayashi, J. Normand, K. Raghavachari, A. Rendell, J.C. Burant, S.S. Iyengar, J. Tomasi, M. Cossi, N. Rega, J.M. Millam, M. Klene, J.E. Knox, J.B. Cross, V. Bakken, C. Adamo,

J. Jaramillo, R. Gomperts, R.E. Stratmann, O. Yazyev, A.J. Austin, R. Cammi, C. Pomelli, J.W. Ochterski, R.L. Martin, K. Morokuma, V.G. Zakrzewski, G.A. Voth, P. Salvador, J.J. Dannenberg, S. Dapprich, A.D. Daniels, O. Farkas, J.B. Foresman, J.V. Ortiz, J. Cioslowski, D.J. Fox, Gaussian Inc, Wallingford, CT, (2009).

[36] A.W. Bauer, M.M. Kirby, J.C. Sherris, et al., Antibiotic susceptibility testing by a standardized single disk method, Am. J. Clin. Pathol. 45 (1966) 493–496.

[37] R. Cruickshank, J. P. Duguid B. P. Marion, R. H. A. Swain, Medicinal Microbiology, twelfth ed., Churchill Livingstone, London, vol. II (1975) 196-202.

[38] C. Perez, M. Pauli, P. Bazerque, An antibiotic essay by the agar well diffusion method, Acta Biol. Med. Exp. 15(1) (1990) 113-115.

[39] M.J. Hearn, M.H. Cynamon, Design and synthesis of antituberculars: preparation and evaluation against Mycobacterium tuberculosis of an isoniazid Schiff base, J. Antimicrob. Chemother. 53 (2) (2004) 185-191.

[40] Z.H. Chohan, S.H. Sumrra, M.H. Youssoufi, T.B Hadda, Metal based biologically active compounds: design, synthesis, and antibacterial/zantifungal/cytotoxic properties of triazole-derived Schiff bases and their oxovanadium (IV) complexes, Eur. J. Med. Chem.45 (7) (2010) 2739-2747.

[41] A. Djedouani, S. Boufas, A. Bendaas, M. Allain, G. Bouet, Bis(3-acetyl-6-methyl-2-oxo-2H-pyran-4-olato) bis (dimethylformamide) nickel(II), Acta Cryst.E65, (2009) m1205.

[42] A. Bouchama, A. Bendaâs, C. Chiter, A. Beghidja, A. Djedouani, Bis(3-acetyl-6-methyl-2-oxo-2H-pyran-4-olato)bis(dimethylformamide)copper(II), Acta Cryst. E63 (2007) m2397.

[43] A. Djedouani, A. Bendaas, S. Bouacida, A. Beghidja, T. Douadi, Bis[3-acetyl-6-methyl-2H-pyran 2,4(3H)dionato]bis(dimethyl sulfoxide)copper(II), Acta Cryst E. E63 (2006) m133–m135.

[44] M.T. Huang, Z.Y. Wang, C.A. Georgiadis, J.D. Laskin, A.H. Conney, Inhibitory effects of curcumin on tumor initiation by benzo[a]pyrene and 7,12-dimethylbenz[a]anthracene, Carcinogenesis 13 (11) (1992) 2183-2186.

[45] P.E. Ikechukwu, P.A. Ajibade, Synthesis, Characterization and Biological Studies of Metal(II) Complexes of (3E)-3-[(2-{(E)-[1-(2,4-Dihydroxyphenyl) ethylidene]amino}ethyl)imino]-1-phenylbutan-1-one Schiff Base, Molecules, 20 (2015) 9788-9802.

[46] R. C. Maurya, B. A. Malik, J. M. Mir, P. K. Vishwakarma, P. S. Jaget, N. Jain, Mixed-ligand Cobalt(II) Complexes of Bioinorganic and Medicinal Relevance, Involving Dehydroacetic Acid and

β-Diketones: Their Synthesis, Hyphenated Experimental-DFT, Thermal and Bactericidal Facets, J. Mol. Struc. 1099 (2015) 266-285.

[47] S. Rahmouni, A. Djedouani, B. Anak, S. Tabti, A. Bendaas, M. ha Bencharif , M. François, S. Fleutot, F. Rabilloud, Synthesis, X-ray crystal structures, electrochemistry and theoretical investigation of a tetradentate nickel and copper Schiff base complexes, J. Mol. Struc. 1148 (2017) 238-246.

[48] R.C. Maurya,B.A.Malik, J.M. Mir, P.K.Vishwakarma, Oxidovanadium(IV) complexes involving dehydroacetic acid and b-diketones of bioinorganic and medicinal relevance: Their synthesis, characterization, thermal behavior and DFT aspects, J. Mol. Struc 1083 (2015) 343–356.

[49] J. M. Mir, R. C. Maurya, D. K. Rajak Bashir A. Malik, P. S. Jaget, N. Jain, A novel Schiff base complex of brain fuel (sugar) coordinated with intelligence mineral (Zn): Synthesis, conjoint DFT-experimental evaluation and super oxide dismutation, Karbala International Journal of Modern Science 3 (2017) 1-12.